Ultrasonics - Sonochemistry 48 (2018) 275–280

Contents lists available at ScienceDirect

Ultrasonics - Sonochemistry

journal homepage: www.elsevier.com/locate/ultson

The effect of high-energy environments on the structure of laccase-polymerized poly(catechol)

Jing Su[a,b], Tarsila G. Castro[b], Jennifer Noro[b], Jiajia Fu[a], Qiang Wang[a], Carla Silva[b], Artur Cavaco-Paulo[a,b,*]

[a] International Joint Research Laboratory for Textile and Fiber Bioprocesses, Jiangnan University, Wuxi 214122, China
[b] Centre of Biological Engineering, University of Minho, Campus de Gualtar, 4710-057 Braga, Portugal

ARTICLE INFO

Keywords:
Catechol
Polymerization
Laccase
Ultrasonic bath
High-pressure homogenizer

ABSTRACT

The laccase polymerization of catechol was performed using different reactors namely a water bath (WB), an ultrasonic bath (US) and a high-pressure homogenizer (HPH). The total content of free OH and the MALDI-TOF spectra of polymers obtained demonstrated that reactions are favored in the presence of high-energy environments. Higher conversion yields and polymerization degrees (DP) were obtained after polymerization using US or HPH. Molecular dynamic simulation studies supported these findings by revealing a more open enzyme active site upon environments with high molecular agitation. The higher mass transport generated by US and HPH is the main feature responsible for a higher substrate accessibility to the enzyme which contributed to produce longer polymers.

1. Introduction

Wastewater discharged from processing industries, like oil refineries and petrochemical, contain dissolved organic pollutants such as phenols and substituted phenolic compounds, which are toxic and hazardous to the environment, unless they are treated properly [1]. A number of technologies have been proposed for the removal of phenolic compounds, like catechol, from wastewater aqueous solutions. These include destructive processes such as chemical oxidation, coagulation, solvent extraction, liquid membrane permeation and adsorption, adsorptive micellar flocculation, ultrafiltration, and biological methods [2]. Although chemical methods are mostly applied, milder reaction conditions (like mild pH and low temperature) are often preferred. Due to their versatile biochemical properties, high protein stability, and breadth of substrate spectrum, laccases are the key promiscuous and environmentally friendly biocatalysts, able to catalyze various aromatic compounds [3]. Previous studies indicate that flavonoids, like catechol, represent important and versatile substrates which are polymerized via laccase-catalyzed oxidation, and the products of reaction are regarded as valuable redox polymers with excellent matrix functionalities applied in several fields [4,5]. In our previous studies we chemically modified laccase from *Myceliophthora Thermophila* by PEGylation with 20 kDa poly(ethylene glycol) methyl ether, and use it to polymerize catechol without solvents addition, using a water bath as reactor device under mild pH conditions (pH 5). We have found that it is possible to control the structure of the poly(catechol) produced by PEGylated laccase polymerization [6]. However, as other studies reported, low polymerization yields were obtained after laccase catalysis in the absence of external stimulus.

Ultrasound has been extensively used in enzyme-catalyzed biotransformations aiming to intensify the reaction processes and obtain higher yield of products in short periods of time [7–10]. Several works have been reporting laccase catalysis assisted by ultrasound however lacking information about the polymer structure obtained using differentiated devices [9,11,12].

High pressure homogenization as well as ultrasound are known to produce cavitation. Comparison studies have been performed between both methods which reveal that hydrodynamic cavitation offers a better control over operating parameters, being more energy-efficient and less sensitive to reactor geometry [13]. However, until now few reports have been presenting the use of hydrodynamic cavitation to assist polymerization being the acoustic cavitation the only tool used for this purpose.

Our aim in this study is to evaluate the role of different high-energy environments on the laccase-assisted polymerization of catechol. For this, three different reactors were used namely a water bath (WB), an ultrasonic bath (US) and a high-pressure homogenizer (HPH). The polymerization was followed during time by UV–Vis spectra analysis of the color change. The produced polymers were characterized by Matrix Assisted Laser Desorption/Ionization-Time of flight Mass spectrometry

* Corresponding author at: Centre of Biological Engineering, University of Minho, Campus de Gualtar, 4710-057 Braga, Portugal
E-mail address: artur@deb.uminho.pt (A. Cavaco-Paulo).

https://doi.org/10.1016/j.ultsonch.2018.05.033
Received 27 February 2018; Received in revised form 21 May 2018; Accepted 28 May 2018
Available online 29 May 2018
1350-4177/

(MALDI-TOF) and ^{1}H NMR. The activity and stability of laccase during processing were evaluated. Molecular dynamic simulations were also conducted to understand the molecular behavior of laccase under high-energy environments.

2. Experimental part

2.1. Materials

Laccase from *Myceliophthora Thermophila* was supplied by Novozymes, Denmark. Catechol, sodium carbonate, Folin-Ciocalteu reagent and MALDI-TOF matrices were purchased from Sigma Aldrich, Spain. Deuterated chloroform and dimethyl sulfoxide were obtained from Cortecnet, France.

2.2. Evaluation of enzyme stability and half-life time quantification

The effect of high-energy environments on the activity and stability of laccase was evaluated. For this, laccase was incubated under the same conditions used for catechol polymerization: the enzyme (100 U/ml) was incubated in acetate buffer (pH = 5) at 40 °C for 2 h using different reactors namely a water bath, an ultrasonic bath and a high-pressure homogenizer. Aliquots of enzyme solution were taken at different periods of incubation and the activity of laccase was measured against ABTS according to the methodology described by Childs and Bardsley [14]. The half-life time of native laccase was calculated according to the Eq. [15]:

$$K = (\ln U_0 - \ln U_t)/t$$

U_0: enzyme activity at time zero;

U_t: enzyme activity at time t;
t: time of incubation;
U: one U is defined as the amount of enzyme that catalyzes the conversion of 1 μmol of substrate (ABTS) per minute.

2.3. Laccase-assisted polymerization of catechol using different reactors

Catechol polymerization was processed by incubating 5 mg/mL of monomer with 100 U/mL laccase in acetate buffer (pH = 5). The reactions were performed in three different reactors namely a water bath (Grant, United Kingdom), an ultrasonic bath (USC600TH, VWR International Ltd., USA; frequency 45 kHz and power of 120 W) and a high-pressure homogenizer (Emulsifex-C3, Avestin, Canada; 500–2000 bar, 50 Hz), at 40 °C for 2 h. During reactions, the temperature of the homogenizer container was monitored using a thermometer. Afterwards the powder was washed with water by centrifugation to remove the maximum amount of protein and dried under vacuum for further ^{1}H NMR and MALDI-TOF characterization.

2.4. UV–Visible spectra analysis

The polymerization was followed by UV–Vis spectroscopy using a 96-quartz microplate reader (Biotek Synergy Mx, Shimadzu, Japan).

2.5. ^{1}H NMR spectra

The precipitates obtained after washing and centrifugation were dissolved in deuterated solvents, DMSO-d_6 and $CDCl_3$, for ^{1}H NMR evaluation. The spectra were acquired in a Bruker Avance III 400 (400 MHz) using the peak solvent as internal reference.

2.6. MASS SPECTRA analysis

The polymers were analyzed by Matrix-Assisted Laser Desorption/Ionization with time-of-flight (MALDI-TOF) using 2,5-dihydroxy benzoic acid (DHB) as the matrix (≥99.5 %). The mass spectra were acquired on an Ultra-flex MALDI-TOF mass spectrophotometer (Bruker Daltonics GmbH) equipped with a 337 nm nitrogen laser. For this, the samples were dissolved in a TA30 (30 % acetonitrile/70 % TFA) solution and mixed with a 20 mg/mL solution of DHB (1:1). Then a volume of 2 μL was placed in the ground steel plate (Bruker part n° 209519) until dry. The mass spectra were acquired in linear positive mode.

2.7. Determination of the total content of free OH

The total content of free OH groups of monomer and polymers was determined before and after polymerization using the Folin-Ciocalteu spectrophotometric method. The monomer and polymer solutions dissolved in DMSO (100 μL) were added to the mixture of Folin-Ciocalteu reagent (500 μL) and distilled water (6 mL), and the mixture was shaken for 1 min. Then Na_2CO_3 solution (15 wt %, 2 mL) was added to the mixture and shaken for 1 min. Later the solution was brought up to 10 mL by adding distilled water. After 2 h, the absorbance was measured at 750 nm (25 °C). The total content of free OH was assessed by plotting a gallic acid calibration curve (from 1 to 1500 μg/ml). The equation of the gallic acid calibration curve was $A = 0.2977c + 0.0368$, and the correlation coefficient was $r^2 = 0.999$.

2.8. Molecular modeling and molecular dynamic simulations

Molecular dynamic (MD) simulations were performed with the native laccase structure originated by homology modelling: the *Myceliophthora thermophila* amino acid sequence was obtained from the Gi number identifier (Gi 10058140) published in 2003 among several laccase structures [16] and accomplished by searching this number on UniProt server [17]. After that, we use the Swiss-model server [18,19] to determine the laccase 3D structure under study, building a model from the most similar laccase template, *Melanocarpus albomyces*, [20] with 75 % of similarity.

Laccase was modelled with the simple point charge (SPC) water model in an octahedral box with a hydration layer of at least 1.5 nm between the peptide and the walls. Na^+ ions were added to neutralize the simulation boxes. Three stages of energy minimization were performed using a maximum of 50,000 steps with steepest descent algorithm, due to the size of the system. Position restraints were applied in all heavy atom at the first step, followed by position restraints in the main chain atoms for the second step, and no restraints were used for the last step of energy minimization. The systems were initialized in a NVT ensemble, using Berendsen [21] algorithm, with the coupling constant $\tau_T = 0.10$ ps, to control temperature at 310 K (40 °C) and simulate the experimental conditions used. After that, a NPT initialization step was performed, with V-rescale [22] and Parrinello-Rahman barostat [23] algorithms to couple temperature and pressure at 313 K and 1 atm, respectively. The following coupling constants were considered: $\tau_T = 0.10$ ps and $\tau_P = 2.0$ ps. Position restraints (with force constant of 1000 kJ·mol^{-1}·nm^{-2}) were applied to all protein heavy atoms in NVT initialization, and in the main chain in NPT step. The positions of copper atoms in the active site were frozen to maintain the coordination with histidine. Simulated Annealing [24,25] method was performed during 10 ns to gently carry the system from 36 to 70 °C, simulating the experimental temperature conditions. After this procedure, one of the frames at 36 °C and other at 70 °C were submitted to classical molecular dynamics during 30 ns, without position restraints, and with the same NPT ensemble described above. All simulations were performed using the GROMACS 4.5.4 version [26–28], within the GROMOS 54a7 force field (FF) [29]. The Lennard-Jones interactions were truncated at 1.4 nm and using particle-mesh Ewald (PME) [30] method for electrostatic interactions, also with a cut-off of 1.4 nm. The algorithm LINCS [31,32] was used to constrain the chemical bonds of the enzyme and the algorithm SETTLE [33] in the case of water. From MD simulations, we computed the middle structure at 36 °C and 70 °C,

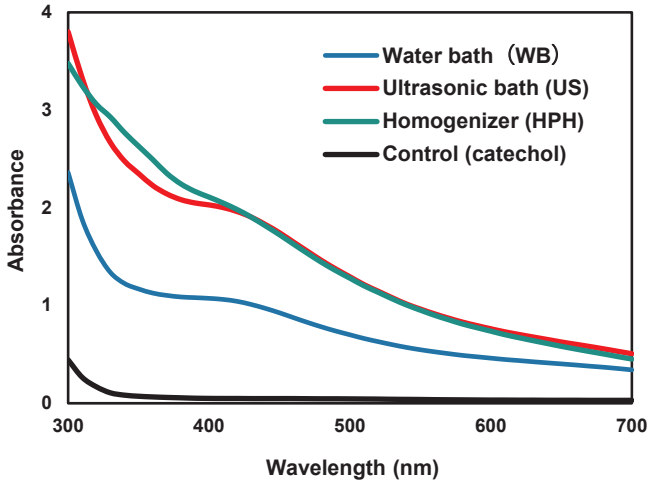

Fig. 1. UV–Visible spectra of poly(catechol) after polymerization with 100 U/mL$_{laccase}$ for 2 h at 40 °C using: water bath (blue line); ultrasonic bath (red line); high-pressure homogenizer (green line); control (buffer + catechol, without laccase) (black line) (the controls performed on the 3 reactors present similar spectral behavior). (For interpretation of the references to colour in this figure legend, the reader is referred to the web version of this article.)

through a single linkage analysis, implemented on GROMACS [26]. This technique adds structures that are below a RMSD (Root Mean Square Deviation) cut-off, generating more or less populated clusters and, within the largest cluster, it finds a middle structure that is the most representative of the whole simulation. We look at these central structures to analyze the differences in the active site, in both cases.

Molecular dynamics/docking data is shown in Supporting Information to provide additional information about the *Myceliophthora thermophila* active site and its interactions with catechol at target temperatures.

3. Results and discussion

3.1. Characterization of the poly(catechol)

We have previously set-up the optimal conditions for the laccase-assisted polymerization of catechol using a water bath. The optimal conditions were considered herein for the polymerization using the high-pressure homogenizer. During catechol polymerization, the changes in the UV–Visible region were recorded to follow the reaction along time. Fig. 1 presents the spectra, after saturation, of poly(catechol) after 2 h of polymerization using different reactors. All spectra present a typical peak at 300 nm which intensity increases after polymerization, probably due to a new molecular arrangement and polymer formation. The intensity increment is more evident for the solutions polymerized under high-energy environments (US and HPH). Respecting to control (conducted in the same conditions without enzyme), a new peak can be depicted at around 430 nm for all the polymer solutions. The increase of absorption is directly related with the amount of polymers in solution which is remarkable higher for samples polymerized in the presence of high-energy environments.

In order to predict the influence of high-energy environments on the polymer structure of the newly formed poly(catechol), we measured the total content of free OH in the polymer mixtures. As shown in Table 1, when ultrasound and high-pressure homogenization are applied, a lower content of free OH is observed, confirming a higher amount of polymer produced. The positive role of cavitation was not only perceived for the improvement of the conversion yields but was also effective on producing polymers with high molecular weight, as demonstrated by MALDI-TOF results (Fig. 2). Despite the decrease of the total free OH observed, the spectra of products obtained using the WB show the formation of polymers with low average molecular weight. It is expectable that the reduced time of incubation (2 h) will give rise, in this case, to low amount of polymer which is hard to ionize during MALDI-TOF evaluation. The spectra that resulted from catalysis using both US and HPH, show average polymerization degrees of 8 and 6, respectively for US and HPH, while for the water bath is 5. The effects resulting from acoustic and hydrodynamic cavitation are mainly high levels of transport. In both cases, sonication is most likely affected by physical rather than chemical activation, by increasing the mass transfer and, by sweeping the polymer surface, creating more propagation sites [34]. In the case of hydrodynamic cavitation, considering the data obtained, one can predict a more homogeneous chain growth, hence a narrower distribution of the molecular weight (Fig. 2). A comparison between both high energy devices, ultrasonic bath and homogenizer, must be considered for a further practical application. According to reported in literature the homogenizer presents some advantages in large-scale operation relatively to its counterpart. It is proved to be more energy-efficient, easier to generate and less sensitive to the geometry of the vessel [13]. The energy input required by the hydrodynamic cavitation reactor is lower since it converts its pressure energy into kinetic energy and its distribution is more homogeneous allowing a continuous operation [35].

Table 1
Laccase-assisted polymerization of catechol using different reactors: water bath (WB), ultrasonic bath (US) and high-pressure homogenizer (HPH) (conversion yield, total content of free OH, and Mn, Mw).

	Reactors		
	Water bath (WB)	Ultrasonic bath (US)	High-pressure homogenizer (HPH)
Conversion yield (%)$^{\Delta}$	73.75	83.60	86.20
TCFOH$^{\cdot}$	0.55	0.29	0.39
Mn, Mw*	547, 560	818, 836	609, 689

* Calculated by MALDI-TOF spectra analysis.
$^{\Delta}$ Calculated by polymer weighting.
$^{\cdot}$ The values are normalized considering the total content of free OH of catechol as 1.00 (100 %).

The differentiated polymerization observed when high-energy reactors were used was also confirmed by ^{1}H NMR analysis (Fig. S1). ^{1}H NMR spectra recorded in DMSO-d$_6$ showed no significant differences between the structure of the polymers obtained using water bath, ultrasonic bath or high-pressure homogenizer. However, when the spectra were recorded in $CDCl_3$ (Fig. S1), we observed significant polymer solubility differences depending on the reactor used. The starting material, catechol, was highly soluble in this solvent, but the polymers produced using ultrasound and homogenizer were extremely insoluble. Considering that only unreacted catechol is solubilized in $CDCl_3$, it was possible to compare its amount in all spectra. The amount of unreacted catechol is higher for samples incubated using a water bath followed by ultrasonic bath and high-pressure homogenizer. Taking this into consideration we might conclude that when the polymerization is conducted under high-energy environments, either acoustic or hydrodynamic cavitation, a high conversion of catechol into poly(catechol) occurred.

3.2. Laccase activity and stability during catalysis

Proteins are sensitive to high temperatures and it is expected that either ultrasound or high-pressure homogenization might lead to activity loss [9,36,37]. To predict the effect of the different high-energy environments used, the activity of laccase was evaluated during processing. Fig. 3 shows the residual activity of laccase when processed using different reactors. The results obtained show that after incubation

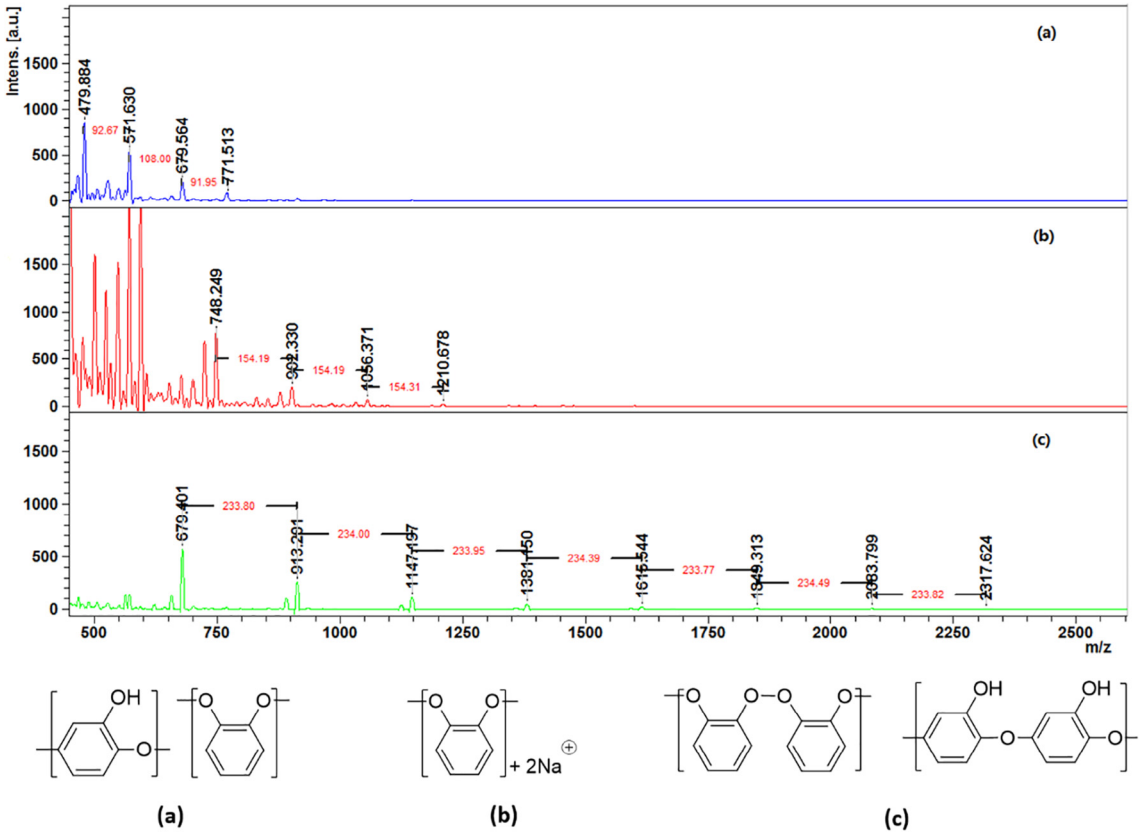

Fig. 2. MALDI-TOF spectra of poly(catechol) after polymerization with 100 U/mL$_{laccase}$ for 2 h at 40 °C using: **(a)** water bath; **(b)** ultrasonic bath and **(c)** high-pressure homogenizer; at the top-down image are represented the possible polymer structures:(**a**: [M/(M-O)]; **b**: [M + 2Na$^+$]; **c**: [2M + Na$^+$-5H$^+$], M represents the catechol monomeric unit).

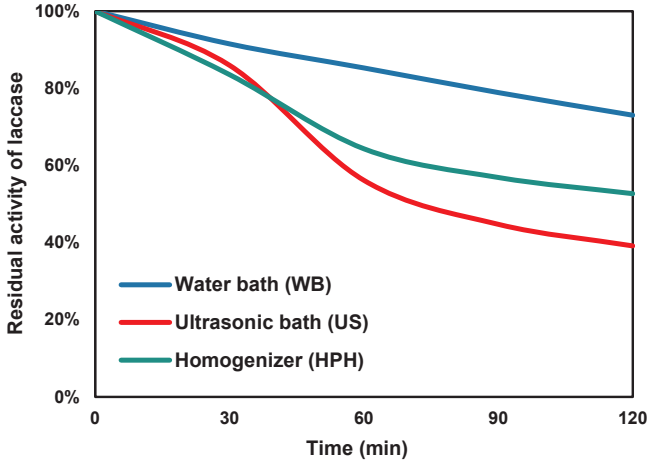

Fig. 3. Residual activity of laccase (40 °C, pH 5) using: water bath (WB) (blue line); ultrasonic bath (US) (red line) and high-pressure homogenizer (HPH) (green line); the measurements were performed until enzyme loosed 50 % of the initial activity; for all conditions, the initial laccase activity was considered as 100 %. (For interpretation of the references to colour in this figure legend, the reader is referred to the web version of this article.)

Table 2
Half-life time of laccase incubated in different reactors.

	Water bath (WB)	Ultrasonic bath (US)	High-pressure homogenizer (HPH)
Half-life time (h)	41.30	1.35	2.50

in the water bath the enzyme retains almost 80 % of its initial activity. When high-energy environments (US or HPH) are applied, the half-life of the enzyme is greatly reduced (Table 2). However, since polymerization occurs in the first 0,5–1 h of incubation, the activity loss will not restrict the final amount of poly(catechol) produced.

3.3. Simulation of laccase behavior under heating conditions

Extreme local temperature and pressure are properties generally related with the cavitation phenomena which might affect enzymatic activity. The cavitation reactors used herein are not exception and an increase of the local temperature was observed during time by thermometer monitoring. For this reason, it was imperative to simulate the behavior of the enzyme in conditions of heating increase. Simulated Annealing (SA) [24,25] method was performed to study the behavior of laccase under heating. This was performed by increasing the temperature during Molecular Dynamic (MD) simulations. The temperature was increased from 310 to 344 K (36 °C–70 °C), in 10 ns. Afterwards the simulation was conducted 30 ns with the initial structure at 36 °C and the last frame at 70 °C, from SA method. Fig. 4 highlights the active site of the middle structure of laccase under different temperatures.

After simulation one can infer that at 36 °C, the enzyme is very stable, with the typical front access to the T1 copper in the active site. At 70 °C, the active pocket is more opened in several directions, which is easily observed analyzing both representations. The accesses from back, top and front to the T1 copper atom, facilitate the catechol entrance and the polymerization process. At higher temperatures, well-defined cavities can be observed leading to a greater facility of the substrate to enter the cavity and reach the copper. These data allowed us to speculate that enlarged catalytic pocked might favor the formation of larger polymer and/or the formation of different types of poly

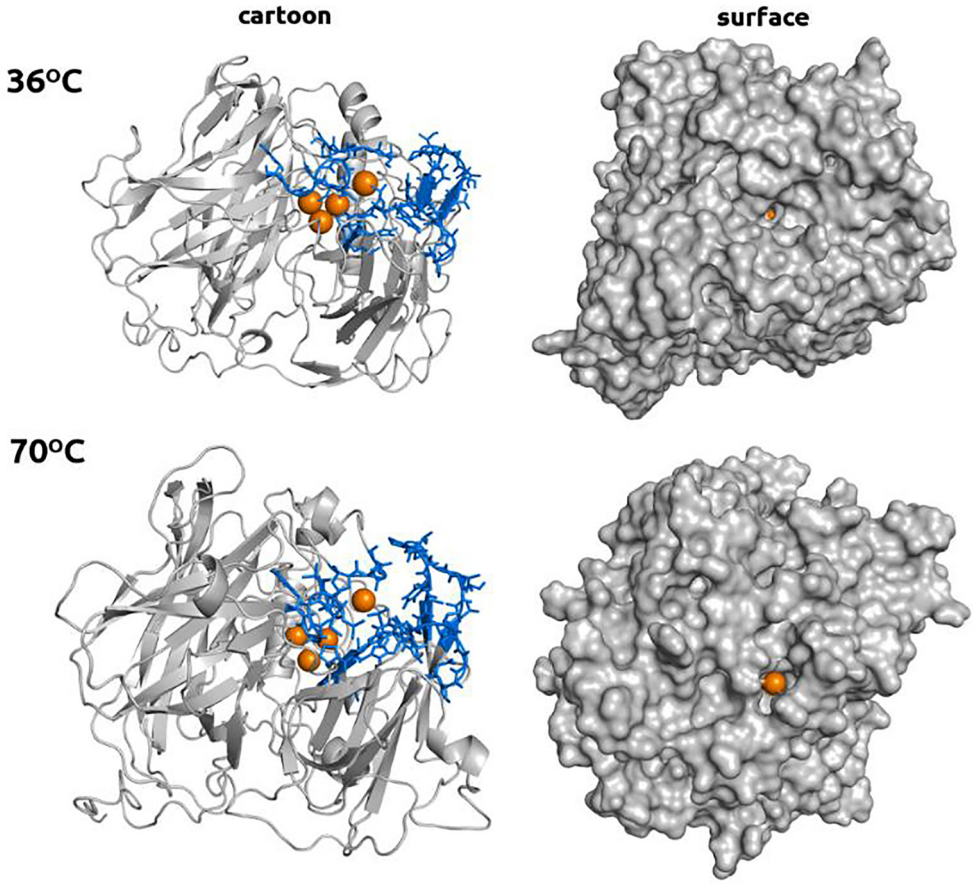

Fig. 4. Middle structures of laccase at 36 °C and 70 °C in cartoon (left) and surface (right) representations; active site and cavities, for catechol access to the T1 copper site, are highlighted using amino acid side chains in blue or the surface shape; laccase is represented in grey and copper atoms in orange.

(catechol) (as shown in Fig. 2).

Our experimental data shows that under high-energy environments the enzyme is active during time enough to process the polymerization of the substrate, but the tendencies of enlargement of the catalytic pocket might also lead later to a progressive loss of enzyme activity.

Further molecular dynamics/docking data (Figs. S2 and S3) suggest that apparently at 40 °C catechol stays closer to T1 copper and at 70 °C it stays close to T2/T3 site, which would be consistent with the loss of enzyme activity [38], but the polymers are formed anyway. Molecular dynamic tools used herein seems do not explain completely our system. We do think that the increased high mass transport effects provided by ultrasound and high-pressure homogenization will contribute to a faster kinetics and increased molecular weight of the poly(catechol) formed.

4. Conclusions

The role of high-energy environments on the polymerization of catechol by laccase was evaluated. The data obtained revealed that a higher mass transport occurring in US and HPH improves greatly the polymerization conversion yields. Longer polymers are obtained especially when the reaction is conducted in a high-pressure homogenizer (HPH). The decrease of enzyme activity observed during processing did not hampered the polymerization since it occurs mainly in the first half-hour where the catalyst maintained 80 % of its residual activity. One can also highlight that heating generated by high-energy environments favored the polymerization process as we confirmed by molecular dynamic simulations.

Acknowledgements

This study was supported by Chinese Government Scholarship under China Scholarship Council (No. 201606790036) and Chinese Foundation Key projects of governmental cooperation in international scientific and technological innovation (No. 2016 YFE0115700) and by the Portuguese Foundation for Science and Technology (FCT) under the scope of the strategic funding of UID/BIO/04469/2013 unit and COMPETE 2020 (POCI-01-0145-FEDER-006684) and BioTecNorte operation (NORTE-01-0145-FEDER-000004) funded by European Regional Development Fund under the scope of Norte2020 – Programa Operacional Regional do Norte. Tarsila Castro thanks the senior position funded by the European Union through the European Regional Development Fund (ERDF) under the Competitiveness Operational Program (COP-A1.1.4-E-2015 nr.30/01.09.2016). Access to computing resources funded by the Project “Search-ON2: Revitalization of HPC infrastructure of UMinho” (NORTE-07-0162-FEDER-000086), co-funded by the North Portugal Regional Operational Programme (ON.2 – O Novo Norte), under the National Strategic Reference Framework (NSRF), through the European Regional Development Fund (ERDF), is also gratefully acknowledged. Jennifer Noro also thanks to FCT-Fundação para a Ciência e a Tecnologia for funding her scholarship (SFRH/BD/121673/2016).

References

[1] A. Mandal, K. Ojha, A.K. De, S. Bhattacharjee, Removal of catechol from aqueous solution by advanced photo-oxidation process, Chem. Eng. J. 102 (2004) 203–208.
[2] K. Shakir, H.F. Ghoneimy, A.F. Elkafrawy, S. Beheir, M. Refaat, Removal of catechol from aqueous solutions by adsorption onto organophilic-bentonite, J. Hazard. Mater. 150 (2008) 765–773.

[3] P.J. Strong, H. Claus, Laccase: a review of its past and its future in bioremediation, Crit. Rev. Environ. Sci. Technol. 41 (2011) 373–434.
[4] S. Witayakran, Laccase in Organic Synthesis and its Applications, 2008.
[5] J. Su, J. Fu, Q. Wang, C. Silva, A. Cavaco-Paulo, Laccase: a green catalyst for the biosynthesis of poly-phenols, Crit. Rev. Biotechnol. 1–14 (2017).
[6] J. Su, J. Noro, A. Loureiro, M. Martins, N.G. Azoia, J. Fu, Q. Wang, C. Silva, A. Cavaco-Paulo, PEGylation greatly enhances laccase polymerase activity, ChemCatChem 9 (2017) 3888–3894.
[7] P.R. Gogate, A.M. Kabadi, A review of applications of cavitation in biochemical engineering/biotechnology, Biochem. Eng. J. 44 (2009) 60–72.
[8] P.B. Subhedar, P.R. Gogate, Enhancing the activity of cellulase enzyme using ultrasonic irradiations, J. Mol. Catal. B: Enzym. 101 (2014) 108–114.
[9] M.M. Delgado-Povedano, M.D. Luque de Castro, A review on enzyme and ultrasound: a controversial but fruitful relationship, Anal. Chim. Acta 889 (2015) 1–21.
[10] S.V. Sancheti, P.R. Gogate, Intensification of heterogeneously catalyzed Suzuki-Miyaura cross-coupling reaction using ultrasound: understanding effect of operating parameters, Ultrason. Sonochem. 40 (2018) 30–39.
[11] X. Yuan, X. Li, X. Zhang, Z. Mu, Z. Gao, L. Jiang, Z. Jiang, Effect of ultrasound on structure and functional properties of laccase-catalyzed α-lactalbumin, J. Food Eng. 223 (2018) 116–123.
[12] B. Kwiatkowska, J. Bennett, J. Akunna, G.M. Walker, D.H. Bremner, Stimulation of bioprocesses by ultrasound, Biotechnol. Adv. 29 (2011) 768–780.
[13] V.S. Moholkar, P. Senthil Kumar, A.B. Pandit, Hydrodynamic cavitation for sonochemical effects, Ultrason. Sonochem. 6 (1999) 53–65.
[14] R.E. Childs, W.G. Bardsley, The steady-state kinetics of peroxidase with 2,2'-azino-di-(3-ethyl-benzthiazoline-6-sulphonic acid) as chromogen, Biochem. J. 145 (1975) 93–103.
[15] A. Zille, T. Tzanov, G. Guebitz, A. Cavaco-Paulo, Immobilized Laccase for Decolourization of Reactive Black 5 Dyeing Effluent, 25 (2003) 1473-1477.
[16] B. Valderrama, P. Oliver, A. Medrano-Soto, R. Vazquez-Duhalt, Evolutionary and structural diversity of fungal laccases, Antonie Van Leeuwenhoek 84 (2003) 289–299.
[17] A. Bateman, M.J. Martin, C. O'Donovan, M. Magrane, E. Alpi, R. Antunes, B. Bely, M. Bingley, C. Bonilla, R. Britto, B. Bursteinas, H. Bye-Ajee, A. Cowley, A. Da Silva, M. De Giorgi, T. Dogan, F. Fazzini, L.G. Castro, L. Figueira, P. Garmiri, G. Georghiou, D. Gonzalez, E. Hatton-Ellis, W. Li, W. Liu, R. Lopez, J. Luo, Y. Lussi, A. MacDougall, A. Nightingale, B. Palka, K. Pichler, D. Poggioli, S. Pundir, L. Pureza, G. Qi, S. Rosanoff, R. Saidi, T. Sawford, A. Shypitsyna, E. Speretta, E. Turner, N. Tyagi, V. Volynkin, T. Wardell, K. Warner, X. Watkins, R. Zaru, H. Zellner, I. Xenarios, L. Bougueleret, A. Bridge, S. Poux, N. Redaschi, L. Aimo, G. ArgoudPuy, A. Auchincloss, K. Axelsen, P. Bansal, D. Baratin, M.C. Blatter, B. Boeckmann, J. Bolleman, E. Boutet, L. Breuza, C. Casal-Casas, E. De Castro, E. Coudert, B. Cuche, M. Doche, D. Dornevil, S. Duvaud, A. Estreicher, L. Famiglietti, M. Feuermann, E. Gasteiger, S. Gehant, V. Gerritsen, A. Gos, N. Gruaz-Gumowski, U. Hinz, C. Hulo, F. Jungo, G. Keller, V. Lara, P. Lemercier, D. Lieberherr, T. Lombardot, X. Martin, P. Masson, A. Morgat, T. Neto, N. Nouspikel, S. Paesano, I. Pedruzzi, S. Pilbout, M. Pozzato, M. Pruess, C. Rivoire, B. Roechert, M. Schneider, C. Sigrist, K. Sonesson, S. Staehli, A. Stutz, S. Sundaram, M. Tognolli, L. Verbregue, A.L. Veuthey, C.H. Wu, C.N. Arighi, L. Arminski, C. Chen, Y. Chen, J.S. Garavelli, H. Huang, K. Laiho, P. McGarvey, D.A. Natale, K. Ross, C.R. Vinayaka, Q. Wang, Y. Wang, L.S. Yeh, J. Zhang, UniProt: the universal protein knowledgebase, Nucl. Acids Res. 45 (2017) D158–D169.
[18] M. Biasini, S. Bienert, A. Waterhouse, K. Arnold, G. Studer, T. Schmidt, F. Kiefer, T.G. Cassarino, M. Bertoni, L. Bordoli, T. Schwede, SWISS-MODEL: modelling protein tertiary and quaternary structure using evolutionary information, Nucl. Acids Res. 42 (2014).
[19] L. Bordoli, F. Kiefer, K. Arnold, P. Benkert, J. Battey, T. Schwede, Protein structure homology modeling using SWISS-MODEL workspace, Nat. Protoc. 4 (2009) 1–13.
[20] N. Hakulinen, M. Andberg, J. Kallio, A. Koivula, K. Kruus, J. Rouvinen, A near atomic resolution structure of a Melanocarpus albomyces laccase, J. Struct. Biol. 162 (2008) 29–39.
[21] H.J.C. Berendsen, J.P.M. Postma, W.F.V. Gunsteren, A. DiNola, J.R. Haak, Molecular dynamics with coupling to an external bath, J. Chem. Phys. 81 (1984) 3684–3690.
[22] G. Bussi, D. Donadio, M. Parrinello, Canonical sampling through velocity rescaling, J. Chem. Phys. 126 (2007) 014101.
[23] R. Martonak, A. Laio, M. Parrinello, Predicting crystal structures: the Parrinello-Rahman method revisited, Phys. Rev. Lett. 90 (2003) 4.
[24] J.-Y. Yi, J. Bernholc, P. Salamon, Simulated annealing strategies for molecular dynamics, Comput. Phys. Commun. 66 (1991) 177–180.
[25] R.C. Bernardi, M.C. Melo, K. Schulten, Enhanced sampling techniques in molecular dynamics simulations of biological systems, Biochim. Biophys. Acta 2015 (1850) 872–877.
[26] S. Pronk, S. Páll, R. Schulz, P. Larsson, P. Bjelkmar, R. Apostolov, M.R. Shirts, J.C. Smith, P.M. Kasson, D. van der Spoel, B. Hess, E. Lindahl, GROMACS 4.5: a high-throughput and highly parallel open source molecular simulation toolkit, Bioinformatics 29 (2013) 845–854.
[27] B. Hess, C. Kutzner, D. van der Spoel, E. Lindahl, GROMACS 4: algorithms for highly efficient, load-balanced, and scalable molecular simulation, J. Chem. Theory Comput. 4 (2008) 435–447.
[28] D.v.d. Spoel, E. Lindahl, B. Hess, A.R.v. Buuren, E. Apol, P.J. Meulenhoff, P. Tieleman, A.L.T.M. Sjibers, K.A. Feenstra, R.v. Drunen, H.J.C. Berendsen, Gromacs user manual version 4.5, in, 2010.
[29] N. Schmid, A.P. Eichenberger, A. Choutko, S. Riniker, M. Winger, A.E. Mark, W.F. van Gunsteren, Definition and testing of the GROMOS force-field versions 54A7 and 54B7, Eur. Biophys. J. 40 (2011) 843–856.
[30] T. Darden, D. York, L. Pedersen, Particle mesh Ewald: an N·log(N) method for Ewald sums in large systems, J. Chem. Phys. 98 (1993) 10089–10092.
[31] B. Hess, H. Bekker, H.J.C. Berendsen, J.G.E.M. Fraaije, LINCS: a linear constraint solver for molecular simulations, J. Comput. Chem. 18 (1997) 1463–1472.
[32] B. Hess, P-LINCS: a parallel linear constraint solver for molecular simulation, J. Chem. Theory Comput. 4 (2008) 116–122.
[33] D. van der Spoel, P.J. van Maaren, H.J.C. Berendsen, A systematic study of water models for molecular simulation: derivation of water models optimized for use with a reaction field, J. Chem. Phys. 108 (1998) 10220–10230.
[34] G. Cravotto, P. Cintas, Power ultrasound in organic synthesis: moving cavitational chemistry from academia to innovative and large-scale applications, Chem. Soc. Rev. 35 (2006) 180–196.
[35] Y. Tao, J. Cai, X. Huai, B. Liu, Z. Guo, Application of hydrodynamic cavitation to wastewater treatment, Chem. Eng. Technol. 39 (2016) 1363–1376.
[36] E.V. Rokhina, P. Lens, J. Virkutyte, Low-frequency ultrasound in biotechnology: state of the art, Trends Biotechnol. 27 (2009) 298–306.
[37] S.S. Nadar, V.K. Rathod, Ultrasound assisted intensification of enzyme activity and its properties: a mini-review, World J. Microbiol. Biotechnol. 33 (2017) 170.
[38] S.M. Jones, E.I. Solomon, Electron transfer and reaction mechanism of laccases, Cell. Mol. Life Sci. 72 (2015) 869–883.